Arabian Journal for Science and Engineering (2023) 48:14195–14211
https://doi.org/10.1007/s13369-023-08109-9

RESEARCH ARTICLE-CIVIL ENGINEERING

Multifactorial Diffusion of Chloride Ions in Concrete considering the Non-linear Voltage Distortion of Other Species

Enrico Zacchei[1,5] · Juan Lizarazo-Marriaga[3] · Felipe García-Sánchez[4] · Antonio Tadeu[1,2]

Received: 26 July 2022 / Accepted: 13 June 2023 / Published online: 4 August 2023

Abstract
One of the most relevant deterioration mechanisms of reinforced concrete (RC) structures is the corrosion of steel bars by chloride ions. The service life of structures could be extended by monitoring this process. The lack of correlation data between chloride ion diffusion and the electrical field has meant that alternative methods have been developed in this paper. One such method considers diffusivity and the electrical field as non-constant, although they are usually assumed constant, that is, without there being any variability of the involved factors. Therefore, a multi-factorial diffusivity that accounts for the material characteristics and environmental variations is adopted. In addition, an innovative stochastic approach to evaluate the variation of the electrical field while accounting for the non-linear voltage distortion, which considers a multispecies model, has been proposed. More complete 1D/2D electro-mechanical models that are solved by advanced numerical and analytical solutions for electro-mechanical diffusion have been developed. Results show that spatiotemporal numerical models estimate the chloride concentration well, estimating more reliable scenarios to provide information on the safety situation of the structure and make it more sustainable by employing successful preventive treatments.

Keywords Chloride diffusion · Non-constant electric field · Multi-factorial diffusivity · Self-diffusion · Multi-species models

1 Introduction

Old, reinforced concrete (RC) constructions can easily be found worldwide (e.g., viaducts, bridges, stadiums, and buildings), which will probably have structural problems in the near future. One of the main mechanisms causing failure in RC structures is the corrosion of steel rebars by chloride ions [1].

Chloride ions reach the steel rebars by migrating throughout the concrete cementitious matrix from the external environment. The corrosion of the steel reduces the area of the rebars, which weakens the resistance and ductility of the structure [2]. This can lead to structural instability and pose a risk to life [3].

Structures built in aggressive environments such as industrial sites or near the coast are the most exposed to this kind of corrosion phenomenon [4]. Recent studies have shown that the affected structures can be from 1.5 [5] to 4.5 km from the sea [6]. This high figure can be correlated with the wind action as analysed in Ou et al. [7], also reaching 6.5 km from the coastline, where a possible correlation between wind and chloride concentration is shown.

The approach to monitoring the chloride diffusion described in this paper combines some of the key parameters of the diffusion, i.e., the diffusion coefficient (or diffusivity) adjusted for an equivalent electric field. Fick's first and second laws describe the traditional diffusion process. Diffusivity has mainly been used as a constant value without considering the effect on its value of factors like water/cement (w/c) ratio, binding chloride, temperature, concrete aging, and concrete deformation [8, 9]. Only in a few studies is concrete deformation regarded as a factor for diffusivity [10, 11].

✉ Enrico Zacchei
enricozacchei@gmail.com

1 Itecons, Coimbra, Portugal

2 University of Coimbra, CERIS, Department of Civil Engineering, Coimbra, Portugal

3 Departamento de Ingeniería Civil Y Agrícola, Universidad Nacional de Colombia (UNAL), Bogotá, Colombia

4 Department of Civil Engineering, Materials, and Manufacturing, University of Malaga, Calle Dr. Ortiz Ramos S/N, 29071 Málaga, Spain

5 University of Coimbra, CERIS, Coimbra, Portugal

In Yari et al. [12] and Wang et al. [13], the aggregate volume and size effects are also considered to estimate diffusivity for inhomogeneous concrete. Fu et al. [14] introduces a factor that considers the change in pore structure of concrete due to carbonation.

Recent works [2, 15] have focused on some of those aspects of correct diffusivity estimation. In Carrara et al. [15], diffusivity has been separated into four different types (i.e., self-diffusivity, free diffusivity, diffusivity in saturated capillary pores, and solid diffusivity) to calculate which is better to use, whereas in Nguyen et al. [2], diffusivity is considered by using another factor, such as humidity.

All these studies on chloride diffusivity in concrete show how it is necessary to focus on diffusion uncertainties, e.g., material characteristics, models, environmental exposure, and electrical diffusion. Regarding the last parameter, the literature often does not consider electrical diffusion (or electromigration) [1, 16], which means the diffusion process is purely mechanical [17].

Multispecies approaches based on coupling Nernst-Planck models have become popular in the last ten years because they account for all the ionic species that participate in transport, not only chloride ions [16, 18]. Nernst-Planck models include the electric potential gradient as a driven force for ionic transport, which can be used both in modelling chloride tests, such as ASTM C1202 [19], and in chloride self-diffusion in concrete. The electric potential gradient can be described by a linear-ohmic potential and a non-linear voltage distortion [20].

Electro-mechanical chloride ion diffusion can be a tool for structural health monitoring (SHM) systems. Despite the interest in this technique over the last twenty years, there is a gap between the theoretical concept and its application due to low competitiveness and the high cost of sensors [21, 22]. Recent studies refer to SHM systems as "futuristic ideas" for civil engineering [23] and an "emerging topic" since they make it possible to foresee potential damage and identify the real structural behaviour of structures [24].

In some papers, for instance, the electro-mechanical interactions have been studied by adopting carbon nanotubes to monitor a structure's response under loading up to damage through varying the electrical resistance [25]. In Sanchez-Romate et al. [26], some relationships between resistance and deformation were established, showing a quasi-linear trend.

Therefore, this paper sets out a novel study on the electro-mechanical diffusion of chloride ions using non-constant multi-factorial diffusivity. The internal potential (or self-diffusion non-linear voltage distortion) is also considered.

The new contributions, which should complete some aspects partially solved by the authors of this paper (see among others [1, 27–29]), concern:

1. A multi-factorial diffusivity to combine concrete deformation with the chloride ion diffusion. Given that in the literature [25, 30] several studies show a correlation between concrete deformation and the resistivity, it could be possible to find a direct relationship between chloride ion diffusion with resistivity through a diffusivity factor that accounts for the concrete deformation.
2. A non-constant equivalent electrical field and mechanical diffusivity are considered when estimating the fluctuation of the chloride concentration in time t and space x. This analysis is developed using advanced numerical solutions given by Hermite polynomials (HPs) [28, 31] that account for the variable characteristics of the material and external environmental factors.
3. The electrical field correlates with the external ohmic and self-diffusion non-linear voltage distortion. This correlation can be analysed using coupling Nernst-Planck equations. Here, a stochastic analysis was proposed to estimate the variation of the self-diffusion.

From these aspects, it is possible not only to estimate the chloride concentration entirely but also to try to find a correlation between the diffusivity/deformations/electric fields. A correct estimation would avoid useless repairs, treatments, and maintenance strategies with high costs and extended timelines. It is preferable to obtain accurate predictions of the structure response, pre- and post-chloride attacks, during design and construction rather than in-service.

2 Diffusion Model

2.1 Transport of Ions

The following 2D mechanical model describes the diffusion of chloride ions in concrete structures. The chloride concentration, C(x,t), in direction x (i.e., x_1, x_2), and time t in saturated concrete is governed by partial differential equations (PDEs) called Fick's second law [32]:

$$\frac{\partial C(x,\,t)}{\partial t} = \nabla \cdot [D_{cl} \nabla C(x,\,t)] = D_{cl} \frac{\partial^2 C(x,\,t)}{\partial x^2} = D_{cl} \left(\frac{\partial^2 C(x_1,\,t)}{\partial x_1^2} + \frac{\partial^2 C(x_2,\,t)}{\partial x_2^2} \right) \tag{1}$$

where $\nabla C(x,t)$ is the total chloride concentration gradient, and D_{cl} is the diffusivity.

The 1D problem in, let us say, x_1 direction has an analytical solution under the following initial condition (i.c.) a Dirichlet boundary condition (b.c.), respectively:

$$\begin{aligned} &\text{Initial condition (i.c.)}: && C(x_1, 0) = C_0 \\ &\text{Boundary condition (b.c.)}: && C(0, t) = C_s \\ & && C(\infty, t) = C_0(\text{semi} - \text{infinite medium}) \end{aligned} \tag{2}$$

where C_0 and C_s are the inner and surface chloride concentration, respectively [33, 34].

Therefore, the 1D analytical solution is:

$$C(x_1, t) = C_0 + (C_s - C_0)\left[\text{erfc}\left(\frac{x_1}{2\sqrt{D_{cl}\, t}}\right)\right] \tag{3}$$

where erfc(·) is the complementary error function.

The total chloride concentration, C, is divided into free chloride dissolved in a pore solution, C_f, and chloride binding concentration, C_b. As mentioned in [35], the "chloride binding process is very complicated and influenced by various factors, which is generally simplified by the binding adsorption isotherms". Here, the correlations between C_f and C_b at a given temperature are defined by the non-linear Langmuir isotherms [32, 35, 36], thus: $C = C_f + C_b = (\omega_e \times C_f) + \{(\alpha \times C_f)/[1 + (\beta \times C_f)]\}$, where ω_e is the evaporable water content [37] and α and β are material constants (here $\alpha = 11.8$, $\beta = 4.0$ [38]).

C_b is usually assumed to immediately reach equilibrium since the binding process is faster than the diffusion process, therefore it can be considered constant [39]. Also, in [40] there is a linear relation between C and C_f under specific conditions that indicates a small contribution of C_b.

2.2 Inter-Combination of Electric/ Diffusion/Deformation Fields

In this section, three coupled fields are explained: (i) the electric diffusion with the elastic deformation of concrete; (ii) the mechanical diffusion with the elastic deformation of concrete; (iii) the electric diffusion with the mechanical diffusion.

If the first and third fields are known, the second field is often neglected, as already mentioned. The introduction of the three fields, correlated with each other, serves to justify the correlation of the current/diffusion/deformation proposed in this paper.

2.2.1 Coupled Electro–Elastic Fields

The electro-elastic model used to study the composite scheme has been retrieved from the literature [27]. The general relationships which linearly couple the electrical and mechanical fields are expressed as:

$$\sigma_{kj}(x) = c_{kjil}(x)\varepsilon_{il}(x) - e_{kji}(x)E_i(x) \tag{4}$$

$$D_j(x) = e_{jil}(x)\varepsilon_{il}(x) + \varepsilon_{ji}(x)E_i(x) \tag{5}$$

where σ_{kj} and ε_{kj} are the components of the elastic stress and strain tensors, respectively; D_j are the components of the electric flux density vector; E_i are the components of the electric field vector; c_{kjil}, e_{kji} and ϵ_{kj} are the elastic coefficients, piezoelectric coefficients, and the dielectric permittivity coefficients.

The relation between the strain field ε_{kj} and the displacement vectors $u_{k,j}$, $u_{j,k}$, and that between E_k and the gradient of the electric potential, $\nabla\phi_k$, are, respectively:

$$\varepsilon_{kj}(x) = \frac{1}{2}\left(u_{k,j}(x) + u_{j,k}(x)\right) \tag{6}$$

$$E_k(x) = -\nabla\phi_k(x) \tag{7}$$

The fundamental relationships are further subject to conditions of equilibrium and Gauss's law. Under the assumptions of vanishing body forces and vanishing volume charge densities, these governing equations are:

$$\sigma_{kj,j}(x) = 0; \;\; D_{k,k}(x) = 0 \tag{8}$$

Equations (6), (7), subject to assumptions given by Eq. (8), determine the steady-state behaviour of a linear electro-elastic system.

2.2.2 Coupled Mechanical Diffusion-Elastic Fields

As already mentioned, the diffusivity D_{cl} is the key parameter of the diffusion process. It can be considered constant [10], variable [15], or variable multi-factorial [41].

A complete multi-factorial relation was recently proposed by the authors of this paper in [28, 42], and it could be described as:

$$D_{cl} = f_0\left(\frac{w}{c}\right) \times f_1(C_b) \times f_2(T) \times f_3(t) \times f_4(h) \times f_5\left(\varepsilon_{kj}(x)\right) \tag{9}$$

where the factors $f_0(w/c)$, $f_1(C_b)$, $f_2(T)$, $f_3(t)$, and $f_4(h)$ are correlated with the water/cement (w/c) ratio, C_b concentration, temperature T, age t, humidity h, respectively. These factors are not explained here for the sake of brevity, but they can be found in the literature [10, 11, 41].

Equation (9) is an empirical equation that accounts for some external actions (e.g., temperature and humidity) and internal characteristics (e.g., w/c ratio, concrete age) of the used material. In [9], several empirical equations have been listed indicating a possible combination of these factors to estimate a reliable D_{cl}. To the best of the authors' knowledge, Eq. (9) could represent a good model for estimating D_{cl}.

Table 1 Adopted parameters for the mechanical diffusion

Parameter	Value
Inner chloride concentration, C_0	0.50 kg/m^3 [55]
Surface chloride concentration, C_s	1.15 kg/m^3 [54]
Reference factor, f_0(w/c)	4.35 cm^2/year [a]
Binding factor, $f_1(C_b)$	0.41 [b]
Temperature factor, $f_2(T)$	0.84 [c]
Age factor, $f_3(t)$	0.39 [d]
Humidity factor, $f_4(h)$	0.13 [e]
Deformation factor, $f_5(\varepsilon_{kj})$	4.36 (Eq. (10)) [f]
Diffusivity, D_{cl}	0.34 cm^2/year (Eq. 9)

[a]For w/c = 0.50 [11, 63]
[b]For $\omega_e = 0.14$ and $C_f = C_0 + C_s = 1.65$ kg/m^3 [10, 38, 63]
[c]For R = 8.314 J/mol/K, activation energy $E_a = 41.80$ kJ/mol, reference temperature $T_0 = 296.0$ K and T = 293.0 K (i.e., 20.0 ºC) [10, 53]
[d]For reference ager t_{ref} = 28.0 days (i.e., 0.08 years), t = 30.0 years and speed index m = 0.20 [10, 64]
[e]For reference humidity $h_{ref} = 0.75$, spread factor n = 4.0 and h = 0.60 [41, 53]
[f]For ε_{kj} = 1.50‰ (< 5.0‰ [26]), and B = -3.55 × 10^{-3} [11, 21]

Liu et al. (2021) [43] presents a possible relationship between electricity and the concrete age. Indeed, it could be possible to correlate the f_3 factor with E_k. Similarly, here we use the f_5 factor. Particular attention is needed for this since it should allow the correlation of concrete's elastic deformation $\varepsilon_{kj}(x)$ with the chloride diffusion.[1] This factor, shown in [10, 11, 44] is defined as:

$$f_5\left(\varepsilon_{kj}(x)\right) = 1 + \left(B \times \varepsilon_{kj}(x)\right) \tag{10}$$

where B is a coefficient that depends on the material characteristics (Table 1), and experimental laboratory tests have estimated it. In [11], this coefficient has been related to the concrete material regardless of the damage levels. It has been fitted by correlations between strain values and D_{cl} for sound concrete under loadings. It represents the situation where no damage occurs in the elastic state for compressive stresses. The elastic state implies that the pore structure of the concrete changes with the increasing $\varepsilon_{kj}(x)$, and thus D_{cl} values.

It is important to note that Eq. (10) refers only to a low linear compressive deformation. This implies that: (i) the effect of the breakage of electrical pathway due to matrix fracture and damage is not prevalent (e.g., $\varepsilon_{kj}(x) < 5.0$‰) [26, 45]; (ii) a low $\varepsilon_{kj}(x)$ guarantees a linear state [46] during the diffusion, thus also maintaining the validity of Eq. (7).

[1] Note that in this study, we only consider the elastic deformation $\varepsilon_{kj}(x)$ as a constant value in the 2D space x_1-x_2. Therefore $\varepsilon_{kj}(x)$ corresponds to the unique elastic deformation $\varepsilon_{11} = \varepsilon_{22} = \varepsilon$.

2.2.3 Coupled Electro-Mechanical Diffusion Fields

The electro-mechanical model is based on the Nernst-Planck model, which simultaneously describes several ions' mechanical and electric flux, in which chloride is usually of the most interest [1, 16, 39, 47–49].

By extending Eq. (1) and correlating D_{cl} with the absolute value of $|E_k(x)|$ as indicated in [39], the Nernst-Planck equation is:

$$\begin{aligned}\frac{\partial C(x.t)}{\partial t} &= D_{cl}\left[\left(\frac{\partial^2 C(x_1,\,t)}{\partial x_1^2} - \frac{zF\,|E_k\,(x_1)|}{RT}\frac{\partial C(x_1,\,t)}{\partial x_1}\right)\right.\\ &\quad\left.+\left(\frac{\partial^2 C(x_2,\,t)}{\partial x_2^2} - \frac{zF\,|E_k\,(x_2)|}{RT}\frac{\partial C(x_2,\,t)}{\partial x_2}\right)\right]\\ &= D_{cl}\left[\left(\frac{\partial^2 C(x_1,\,t)}{\partial x_1^2} - a(x_1)\frac{\partial C(x_1,\,t)}{\partial x_1}\right)\right.\\ &\quad\left.+\left(\frac{\partial^2 C(x_2,\,t)}{\partial x_2^2} - a(x_2)\frac{\partial C(x_2,\,t)}{\partial x_2}\right)\right]\end{aligned} \tag{11}$$

where z is the valency of the ion, F is the Faraday constant, R is a universal gas constant, and T is the temperature. The a-parameter, considering Eq. (7), is expressed as $a(x) = (z \times F \times |E_k(x)|)/(R \times T)$ [16], which is a function of x-depth due to $E_k(x)$. It can be expressed as a constant or variable (e.g., a × sin(x)) parameter.

The analytical solution of Eq. (11) in x_1 direction, under the same hypotheses used to obtain Eq. (3) plus the a-parameter considered constant, is [16, 39, 50]:

$$\begin{aligned}&C(x_1,\,t)\\ &= C_0 + \left(\frac{C_s - C_0}{2}\right)\left[e^{(a\,x_1)}\mathrm{erfc}\left(\frac{x_1 + aD_{cl}t}{2\sqrt{D_{cl}\,t}}\right) + \mathrm{erfc}\left(\frac{x_1 - aD_{cl}t}{2\sqrt{D_{cl}\,t}}\right)\right]\end{aligned} \tag{12}$$

Equation (11) is usually developed only considering the a-parameter as a constant value, whereas $C_0 = 0$ and $C_s \neq 0$ in Eq. (12). In this respect, Eq. (12) is shown in full.

3 Numerical Solutions

3.1 1D/2D Constant Diffusion

The exact solution of Eq. (1) for $D_{cl} = 1$ by using the Kampé de Fériet polynomials (KDFPs) of non-negative degree n, in direction x_1 and time t (x_1, t ∈ ℝ), is defined by the series [51, 52]:

$$H_n(x_1,\,t) = n!\sum_{r=0}^{\left[\frac{n}{2}\right]}\frac{x_1^{n-2r}\,t^r}{(n-2r)!\,r!} \tag{13}$$

By substituting Eq. (13) in Eq. (1), the following relation is obtained:

$$\frac{\partial}{\partial t} H_n(x_1, t) = \frac{\partial^2}{\partial x_1^2} H_n(x_1, t) \tag{14}$$

$$\begin{aligned} &\text{i.c. : } H_n(x_1, 0) = x_1^n \\ &\text{b.c. : } H_n(0, t) = 0 \end{aligned} \tag{14a}$$

For 2D constant diffusion, Eq. (14) is also valid when t is replaced with x_2. Therefore the boundary conditions are $H_n(x_1, 0) = {x_1}^n$ and $H_n(0, x_2) = 0$.

3.2 1D/2D Non-constant Diffusion

For $D_{cl} \neq 1$, Eq. (13) is not the exact numerical solution of Eq. (1), but it can be used to obtain an approximate solution.

For the 1D model, the ordinary Hermite polynomials (HPs) in x_1 and t are specified by the series [12, 52]:

$$\begin{cases} H_n(x_1) = n! \sum_{r=0}^{\left[\frac{n}{2}\right]} \frac{(2x_1)^{n-2r}(-1)^r}{(n-2r)!r!} & indirection\ x_1 \\ H_n(t) = n! \sum_{r=0}^{\left[\frac{n}{2}\right]} \frac{(2t)^{n-2r}(-1)^r}{(n-2r)!r!} & intime\ t \end{cases} \tag{15}$$

To solve Eq. (1) and Eq. (11) by considering a non-constant D_{cl} and a-parameter, the following conditions are defined:

$$\begin{aligned} &\text{i.c. : } && C(x_{1,m}, 0) = C_0 \\ &\text{b.c. : } && C(0, t_m) = C_s \\ & && C(q \times x_{1,m}, t_m) = C_0 (\text{finite medium}) \end{aligned} \tag{16}$$

where $x_{1,m}$, and t_m are two variables related to position and time, respectively. They must be pre-defined not to generate the arbitrary constants that represent the degrees of freedom associated with i.c. and b.c.; q indicates a multiplier parameter that quantifies the convergence (here, it is assumed $q \approx 20.0$ as already validated by the authors of this paper in [28, 53]).

The 2D model is obtained by adding the following series to Eq. (15) [12, 52]:

$$H_n(x_2) = n! \sum_{r=0}^{\left[\frac{n}{2}\right]} \frac{(2x_2)^{n-2r}(-1)^r}{(n-2r)!\,r!} \tag{17}$$

To solve Eq. (1) and Eq. (11) by considering 2D non-constant D_{cl} and a-parameter, with a fixed t, the conditions are:

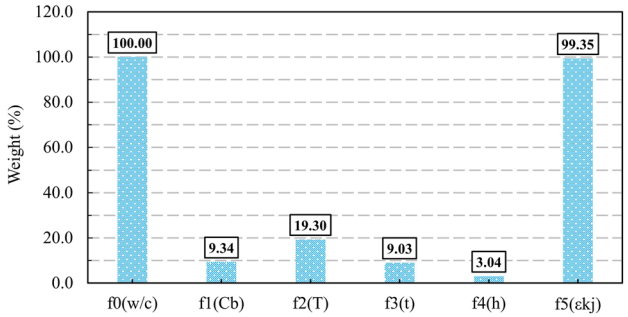

Fig. 1 Weight of each factor with respect to f0 in the mechanical diffusivity

$$\begin{aligned} &\text{i.c. : } && C(x_{1,m}, 0) = C(x_{2,m}, 0) = C_0 \\ &\text{b.c. : } && C(0, t_m) = C_s \\ & && C(q \times x_{1,m}, t_m) = C(q \times x_{2,m}, t_m) = C_0 (\text{finite medium}) \end{aligned} \tag{18}$$

where $x_{2,m}$ is a pre-defined variable related to the position like $x_{1,m}$.

4 Materials and Methods

4.1 Materials

4.1.1 Materials for Mechanical Diffusion

The diffusion process is divided into mechanical and electrical diffusion. Table 1 shows the adopted parameters for mechanical diffusion for ordinary Portland concrete. References justify some used parameters, others are directly calculated; in this respect, they should assume realistic and reliable values.

The external conditions regard a moderate level of aggressiveness (i.e., structures located between 0.10 and 2.84 km from the coast without direct contact with seawater, providing $C_s = 1.15$ kg/m^3 [54]), with temperature T = 20 °C and humidity 60.0% (i.e., h = 0.60). The main internal conditions concern a w/c = 0.50 and $C_0 = 0.50$ kg/m^3 [11, 55].

As mentioned in Sect. 2.2.2, the f_5 factor needs particular attention since it represents the "bridge" between the elastic field and the electro-mechanical diffusion. In this study, the f_5 factor is estimated as 4.36 using the empirical Eq. (10). This factor is difficult to calculate since it correlates the elastic deformation $\varepsilon_{kj}(x)$, due to external actions on an RC element, with the diffusion of chloride ions. In the literature, it can take a value of 1.89 in [56], 3.23 in [17] up to 8.95 in [10, 11], indicating a significant impact on the final D_{cl}, as also shown in Fig. 1.

Figure 1 shows the weight of each multiplicator factor to obtain D_{cl} in this study. The weights are calculated as a percentage (%) with respect to the reference factor f_0.

The weights shown in Fig. 1 help quantify the general role of each factor. Here, f_4 has the lowest weight ($f_4(h) = 3.04\%$) for estimating D_{cl}. Obviously, these weights can vary as a function of the adopted parameters, but generally the predominant factors are f_0 and f_5 [10, 42].

4.1.2 Materials for Electrical Diffusion

The coupled electro-mechanical diffusion fields in Eqs. (11–12) need to be solved for the electrical field, for which an equivalent average value was proposed in the present paper.

In concrete, the electrical field E_k suffers a further internal variation. The variation of E_k in direction x_1 could be formed by an external ohmic potential, which corresponds to the external voltage applied to a sample in a migration test such as the ASTM C1202 [19] and NT492 [57], and a self-diffusion non-linear voltage (or potential) distortion when the pure diffusion occurs.

The method proposed in this paper to calculate an equivalent electric field, E_k, to represent the phenomenon corresponding to the non-linear potential distortion of the ionic self-diffusion, was obtained from a multispecies approach, in which several ions are involved (i.e., Na^+, K^+, and OH^- from the concrete pore solution, and Cl^- penetrating from the outside of the sample). The voltage distortion in concrete subjected to self-diffusion is formed since when all the species start to move, they cannot move freely. This is because they are charged particles that interact with the other species, generating a non-linear voltage distortion.

The theory of the two potential contributions in the x_1 direction are described by [20]:

$$\frac{\partial \phi_k(x_1)}{\partial x_1} = \underbrace{\frac{I}{\left(\sum_i z_i^2\, F^2\, u_i\, c_i\right)}}_{\text{Ohmic potential}} - \underbrace{\frac{\sum_i z_i\, F\, R\, T\, u_i \left(\frac{\partial c_i}{\partial x_1}\right)}{\left(\sum_i z_i^2\, F^2\, u_i\, c_i\right)}}_{\text{Non-linear voltage distortion}} \quad (19)$$

where c_i is the ionic concentration of species i, u_i is the mobility of species i in the pore fluid, I is the external total current density. The other parameters have already been explained.

The method used to obtain a characteristic value and determine which values this electrical field could vary; many simulations were carried out using the multispecies model reported by [58]. In the model, it is assumed that each ion flux is dependent on the other ions; therefore, to maintain the principle of electroneutrality (i.e., ensuring no excess of charge [20]), a non-linear potential distortion is generated even if there is no external E_k. Then, in a self-diffusion condition with no external voltage source, although the external voltage applied is zero, the internal mobility of the species in concrete generates a distortion of the electric potential.

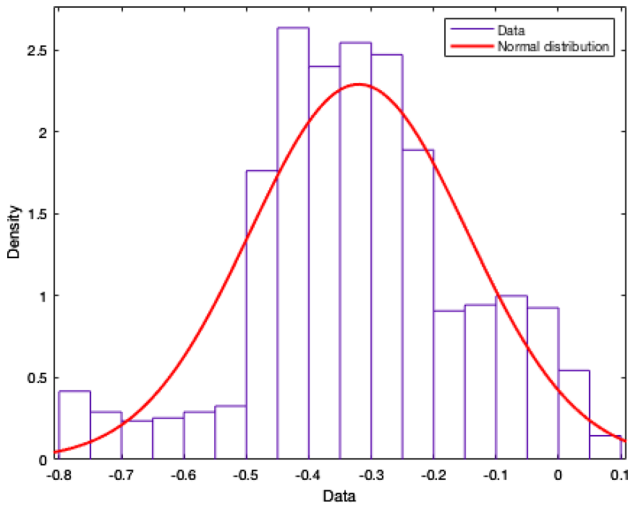

Fig. 2 The electrical field, E_k, developed for self-diffusion conditions (V/m): stochastic data (histograms) and PDF normal distribution (red line)

Table 2 Adopted parameters for electrical diffusion

Parameter	Value
Faraday constant, F	9.65×10^4 C/mol [16]
Electric field, E_k	0.320 ± 0.174 V/m (Fig. 2)
Valency of the ion, z	1.0 [47]
a-parameter	0.13 ± 0.07 cm^{-1} (in Eq. (11))
Electric current, I	2.30×10^{-6} A [a]

[a]Calculated by $I = (A_s \times E_k)/\rho \leq 3.30 \times 10^{-4}$ A (risk-free value for humans [60]), with a square section area $A_s = 3.60 \times 10^{-3}$ m^2 and a specific resistivity $\rho = 5.0 \times 10^2$ ohms × m

About 1100.0 simulations were carried out, randomly varying the diffusion coefficients of the ionic species [59], the chloride binding capacity, and the concentration of the pore solutions of the species involved. Although the potentials generated by the ions coupling would vary in both time and space, for simplicity, here, only the voltage distortion in the central part of a concrete sample (i.e., at 3.0 cm) for several years was considered. Figure 2 shows E_k values by histograms and the fitted probability density function (PDF) by a normal distribution, in which the average value obtained was 0.32 V/m.

Table 2 lists the adopted parameters for electrical diffusion. Some parameters are justified by references, equations, or specific studies, as shown in Fig. 2; therefore, they should take realistic and reliable values. It should be noted that although the coupled mechanical diffusion-elastic and electro-mechanical diffusion fields approaches are related only to chloride ions, the multispecies model (OH^-, Na^+,

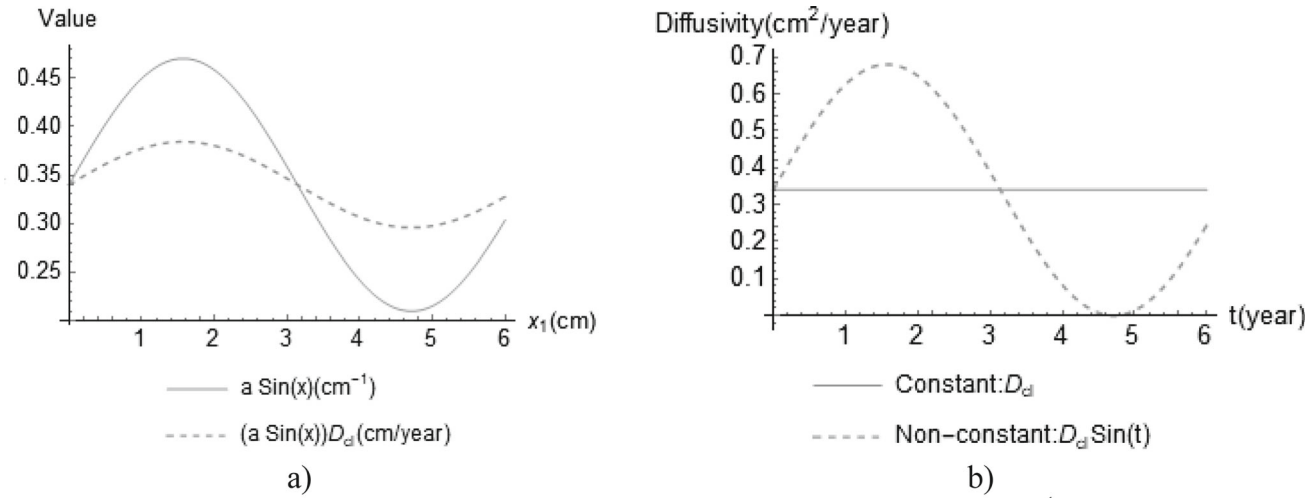

Fig. 3 The sinusoidal trend of **a** non-constant spatial a-parameter ($a = 0.13\ cm^{-1}$); **b** non-constant temporal D_{cl} ($D_{cl} = 0.34\ cm.^2/year$)

K^+, and Cl^-) was used here only to obtain a characteristic value for E_k.

The key parameter in Table 2 is the electrical field E_k since it plays a double role in this study: (i) by conducting a multispecies analysis (Eq. (19)) it is possible to achieve a probabilistic estimate of E_k thus the a-parameter used to carry out Eqs. (11–12) to evaluate the more complete spatial/temporal electro-mechanical diffusion; (ii) from E_k it is possible to obtain an equivalent electrical current, I, for a determined concrete geometry; thus, a possible correlation could be obtained.

Figure 3 shows the trend of the two key parameters that govern the electro-mechanical diffusion process. In Fig. 3a) it is possible to see how D_{cl} affects the electrical a-parameter by reducing its amplitude.

A sinusoidal trend could simulate the trend of the T and h for the mechanical diffusivity, as shown in [41, 42], and for the electrical diffusivity, an alternating current (AC) [60]. Both are usually represented by a sinusoidal function, which is why this function was chosen in this study, although other function types could be adopted [53].

4.2 General Methodology

The general methodology of this study is divided into four main steps, as shown in Fig. 4.

Step 0. The possibility evaluated of finding a correlation between the chloride ion diffusion (mechanical and electrical) and elastic deformation of the material. This step examines research studied in previous works [10, 28, 58, 61, 62].

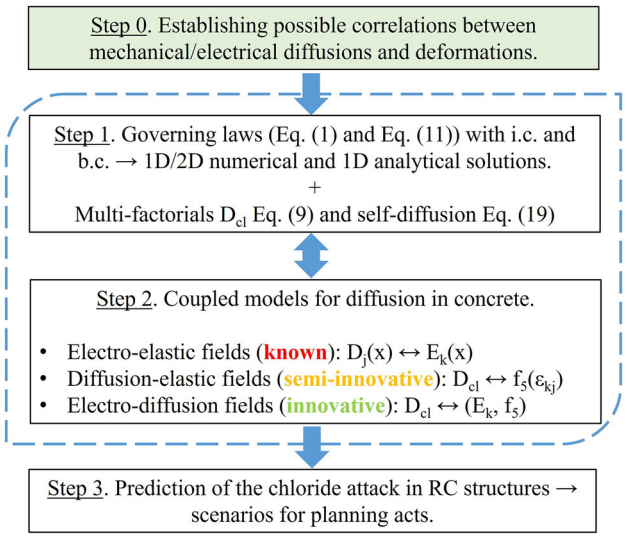

Fig. 4 General methodology of this study

Step 1. In this step, the mathematical models are described considering the mechanical and electrical diffusion. Numerical, modified analytical, and multi-factorial diffusivity solutions are developed. The self-diffusion approach is also proposed.

Step 2. The three coupled fields are defined: (i) electro-elastic, which correlates the electrical field with the material deformations; (ii) diffusion-elastic, which correlates the mechanical diffusion of chloride ions with the material deformations; (iii) electro-diffusion, which correlates the electrical diffusion with the mechanical diffusion. Thus, the correlation of the current/diffusion/deformation is proposed.

Step 3. Finally, the chloride ions concentrations C in concrete in time t and space x by 1D/2D model are estimated. Several factors (mechanicals, electricals, environmental, constitutive) are included. The results thus provide several scenarios to anticipate the chloride ions attack within RC structures.

5 Results and Discussions

5.1 Chloride Concentrations in Concrete

5.1.1 Constant Mechanical and Electro-Mechanical Diffusion

This section shows the mechanical and electro-mechanical chloride ion diffusion, implemented by Mathematica software [51]. Both key parameters (i.e., a-parameter and D_{cl}, shown in Tables 1–2) for estimating the diffusion process are considered constant.

It is therefore possible to develop analytical solutions and quantify the merit of the results since they represent the exact solutions. Analytical solutions should provide reliable results given that D_{cl} and a-parameter have been estimated using more complete models.

Figure 5 shows the 1D chloride diffusion in an RC element by using mechanical (Eq. (3)) and electro-mechanical (Eq. (12)) analytical solutions. The stochastic effect of the E_k shown in Fig. 2 is also evaluated. The curves are calculated for the following values: t = {0.01, 5.0, 10.0, 15.0, 20.0, 25.0} year and x_1 = {0, 1.0, 2.0, 3.0, 4.0, 5.0, 6.0} cm. As the yellow arrows indicate, the curves increase by increasing t and x_1.

In Fig. 5a, c, for the curve t = 0, $C(x_1, t) = C_0$; for this reason, t > 0 is adopted to show a curve. In Fig. 5b, d), the horizontal line corresponds to $x_1 = 0$ when $C(0, t) = C_s$ following Eq. (2).

Two main aspects can be noted. The first concerns the diffusion velocity of the chloride ions by including an electric field. The diffusivity D_{cl} is amplified by the a-parameter that allows the chloride concentration C to reach the depth x_1 = 6.0 cm faster (see black lines in Fig. 5). However, as shown in Fig. 3a), this amplification is not very large (i.e., about 0.38–0.30 = 0.08 cm/year).

The other aspect is the sensitivity of the a-parameter variation, which is more evident for a higher a-parameter (see Fig. 5c–d)). This indicates that it could be challenging to combine the mechanical and the electro-mechanical diffusion for $E_k >> 0$ since the two curves could be very distant from each other. Thus, the two diffusions could not be compatible with each other for monitoring RC structures. Also, it is noted that the electric diffusion affects the total diffusion from t > 2.5 years.

Results of the electro-mechanical model, shown in Fig. 5, controlled by the a-parameter (a function of the electrical field), include, in a simplified macroscopic way, the complex physicochemical phenomena that could be modelled through multi-species approaches in which the ion-ion effects are included, coupling all the species involved, to the charge neutrality. From Fig. 5 it can also be seen that the mechanical model tends to underestimate the penetration of chlorides with respect to what was obtained using the electro-mechanical models. As was expected, this condition is exacerbated as the electric field increases.

Figure 6 shows the 1D mechanical and electro-mechanical diffusion by numerical solutions (i.e., Eq. (1) and Eq. (11) solved with the conditions indicated in Eq. (16)) for a = 0.13 cm^{-1} and D_{cl} = 0.34 cm^2/year.

The numerical solutions for the mechanical diffusion (Fig. 6c–e) are very similar to the analytical solution with an error of ~ 2.0%, whereas for the electro-mechanical solutions (Fig. 6d–f), the approximation is a bit worse (~ 5.0%). This indicates that Eq. (3), as expected, approximates the results quite well, whereas Eq. (12) provides worse results, probably due to double erfc(·). However, a difference between 2.0 and 5.0% can still be considered acceptable. Therefore, this also indicates that the q-parameter (Eq. (16)) adopted for the numerical solutions provides good results.

Also, we can see that numerical solutions have some advantages; for instance, it is possible to plot a curve for x_1 = 0 cm (non-constant outputs in Fig. 6e–f) for non-constant a-parameter and D_{cl} (shown in the following sections).

Figure 7 shows the 2D chloride electro-mechanical diffusion in x_1 and x_2 direction for a = 0.13 ± 0.07 cm^{-1} and for t = {5.0, 25.0} years. The numerical solutions are obtained using Eq. (1) and Eq. (11) with the conditions shown in Eq. (18).

Although the variation of the a-parameter is not very high, it is possible to see its effect on the chloride concentration in the 2D model. In particular, at t = 25.0 years and $x_1 = x_2$ = 6.0 cm (i.e., where steel bars could be placed), the maximum C with a = 0.20 cm^{-1} is greater than the maximum C for a = 0.06 cm^{-1} of 1.06 (see Fig. 7c–d).

When the chloride ions come from two directions, x_1 and x_2, the chloride concentration C is expected to be greater than for unidimensional diffusion. In fact, the ratio between the chloride concentration C is always $C_{2D}/C_{1D} \geq 1.0$. In particular, at 6.0 cm, this ratio is 1.30 for 5.0 years and 1.24 for 25.0 years, in accordance with [53]. This ratio decrease is probably due to a saturation phenomenon that reduces the concrete pores.

5.1.2 Spatial Non-Constant Electro-Mechanical Diffusion

The electro-mechanical diffusion for a non-constant a-parameter is shown in Fig. 8. These numerical results,

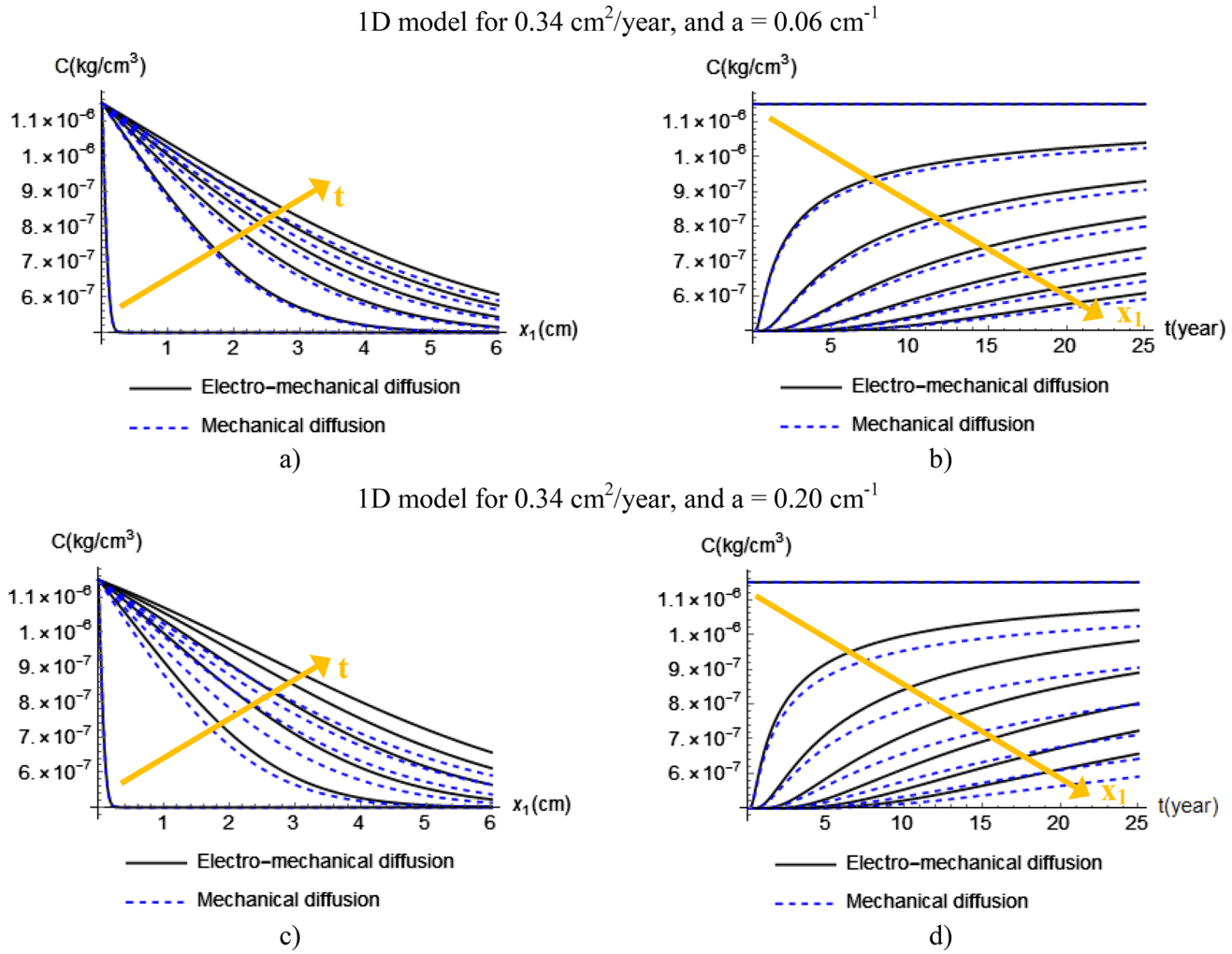

Fig. 5 1D mechanical and electro-mechanical chloride diffusion using analytical solutions for $D_{cl} = 0.34$ cm^2/year and a $= 0.13 \pm 0.07$ cm^{-1}. Curves are plotted for t $= \{0.01, 5.0, 10.0, 15.0, 20.0, 25.0\}$ year and $x_1 = \{0, 1.0, 2.0, 3.0, 4.0, 5.0, 6.0\}$ cm

obtained by developing Eq. (15) with the condition in Eq. (16), account for the variability in the space of the electrical field $E_k(x_1)$. The curves are plotted for different t. Given that variability is spatial, the C curves plotted in time t could not provide significant alterations in this case.

The curves in Fig. 8a) give higher concentration values than those in Fig. 8b). Different from the results with constant a-parameters (Fig. 5a)), here, with a low a-parameter, the chloride concentration increases a little. This estimated rise, at 6.0 cm for 25.0 years, is ~ 1.17; therefore, it is possible to affirm that by considering a-parameter as constant (as usually assumed), the results could provide slightly underestimated values. This effect is due to the fluctuating trend shown in Fig. 3a).

These non-expected results could be correlated to the fact that, for a non-constant D_{cl}, the concentration of the chloride ions in a specific section x_1 is not cumulative; in fact, in general, the physical meaning of the chloride diffusion is that the concentration C increases in t with a constant D_{cl}. When D_{cl} is non-constant, this physical meaning changes; therefore, the mathematical influence of the $a(x_1)$ with a negative sign in Eq. (11) alters the results. Here, the variability in the space of the function a $\times$ Sin(x_1) provides these changes.

5.1.3 Temporal Non-constant Electro-Mechanical Diffusion

The influence of time variability is studied in this section. Figure 9 shows the 1D mechanical and electro-mechanical diffusion for a non-constant diffusivity in t. The curves are obtained by developing Eq. (15) with the conditions indicated in Eq. (16).

The difference between the two models is almost imperceptible; it is very challenging to quantify the chloride ion diffusion by comparing mechanical and electrical models. At t $= 25.0$ years and $x_1 = 6.0$ cm, the electro-mechanical

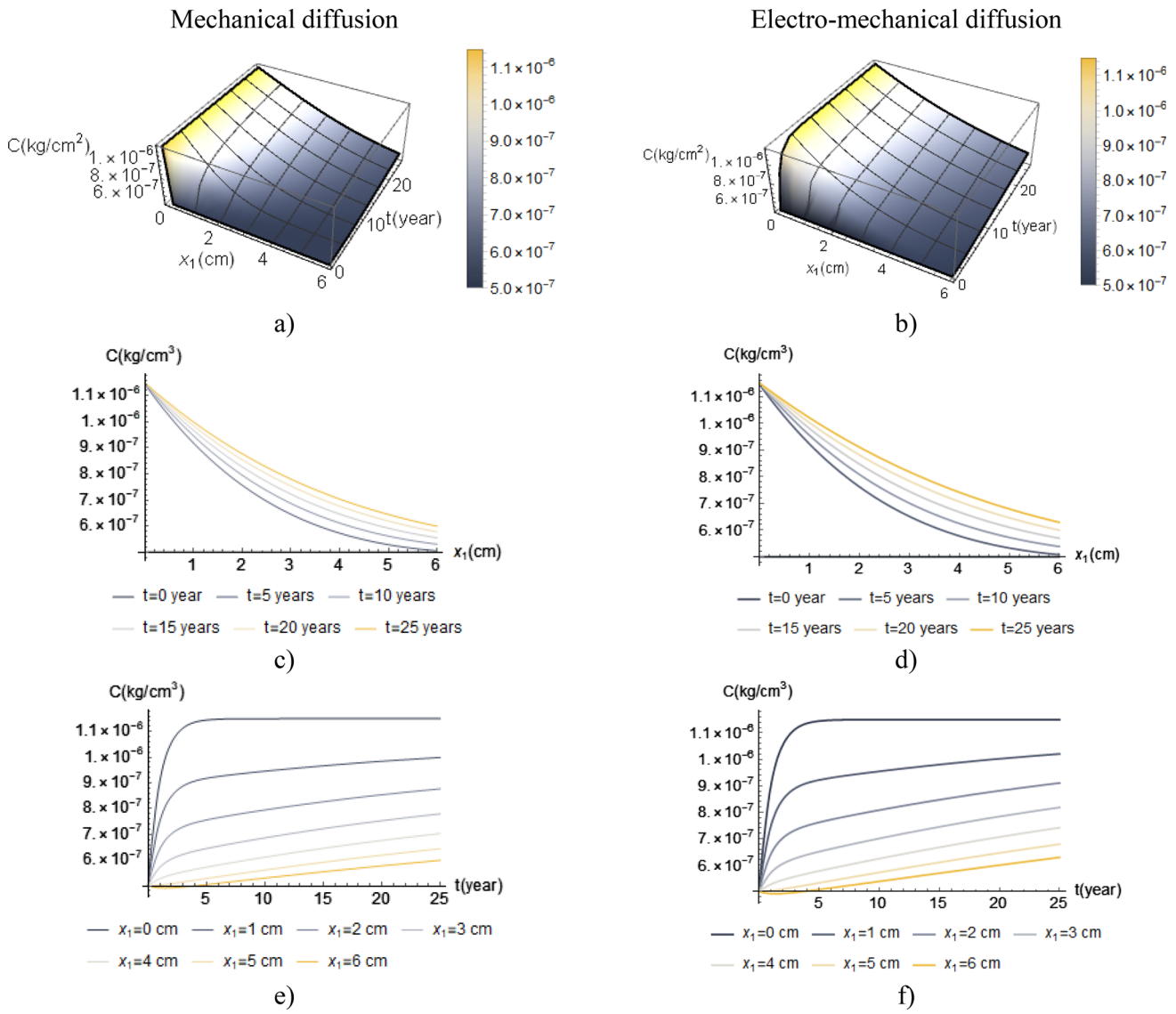

Fig. 6 1D electro-mechanical and mechanical diffusion using numerical solutions ($D_{cl} = 0.34$ cm^2/year and a $= 0.13$ cm.$^{-1}$)

diffusion provides larger values of 1.04 than mechanical diffusion.

Physically, the difference could be small because electrical diffusion is much faster than mechanical diffusion. Moreover, the temporal interval of the diffusivity is different, with the former being studied in seconds and the latter in years.

Evident differences between the chloride concentration in time variability with respect to a constant analysis relate to the oscillations of the curves. In fact, the curves in Fig. 9 are directly affected by the sinusoidal trends shown in Fig. 3b), which could provide values lower than curves for a constant analysis (Fig. 6e–f). In particular, at the point (t = 5.0 years, $x_1 = 3.0$ cm), the difference is 1.05, i.e., the temporal non-constant curve provides a smaller value.

Considering that the model is dynamic, it is possible that for the same depth x_1, the chloride concentration C decreases or increases in t differently for the constant D_{cl}, which increases the concentration C monotonically, as shown in [28]. When a sinusoidal diffusivity is composed of more points placed above the constant D_{cl} (horizontal line in Fig. 3b), the chloride concentration by numerical solution is greater than the chloride concentration by exact solution and vice-versa. This can be also noted in Fig. 11 (shown later), where the difference between C by constant and temporal analysis at 10.0 years (i.e., $10.0 \approx 3\pi$) is greater than at 25.0 years (i.e., $25.0 \approx 8\pi$).

5.1.4 Spatial/Temporal Non-constant Electro-Mechanical Diffusion

This section shows a complete model by considering all dependencies, i.e., the variation of the diffusivity in t, x_1,

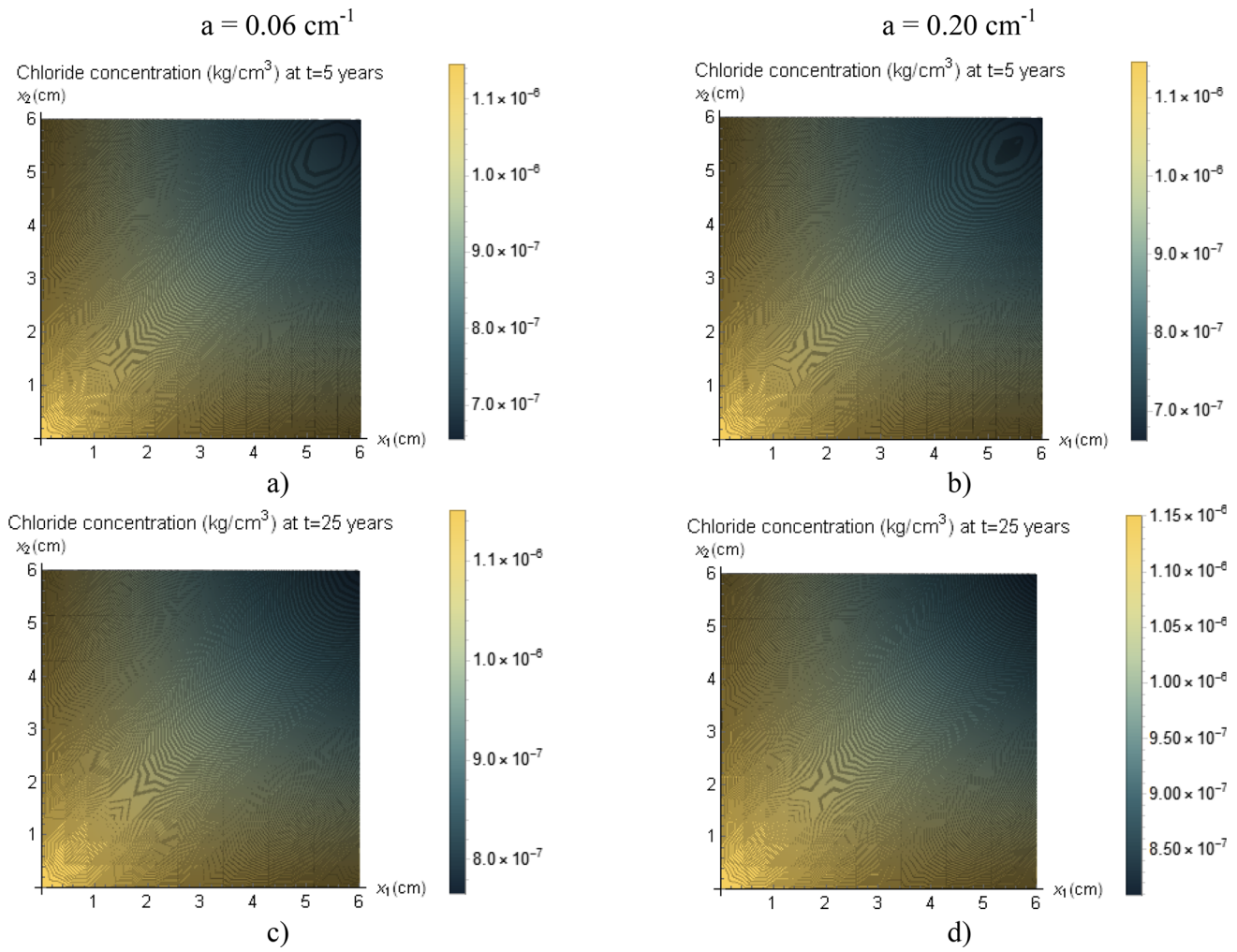

Fig. 7 2D electro-mechanical diffusion in two directions, x_1 and x_2, using numerical solutions for $a = .13 \pm 0.07$ cm^{-1} at 5.0 and 25.0 years

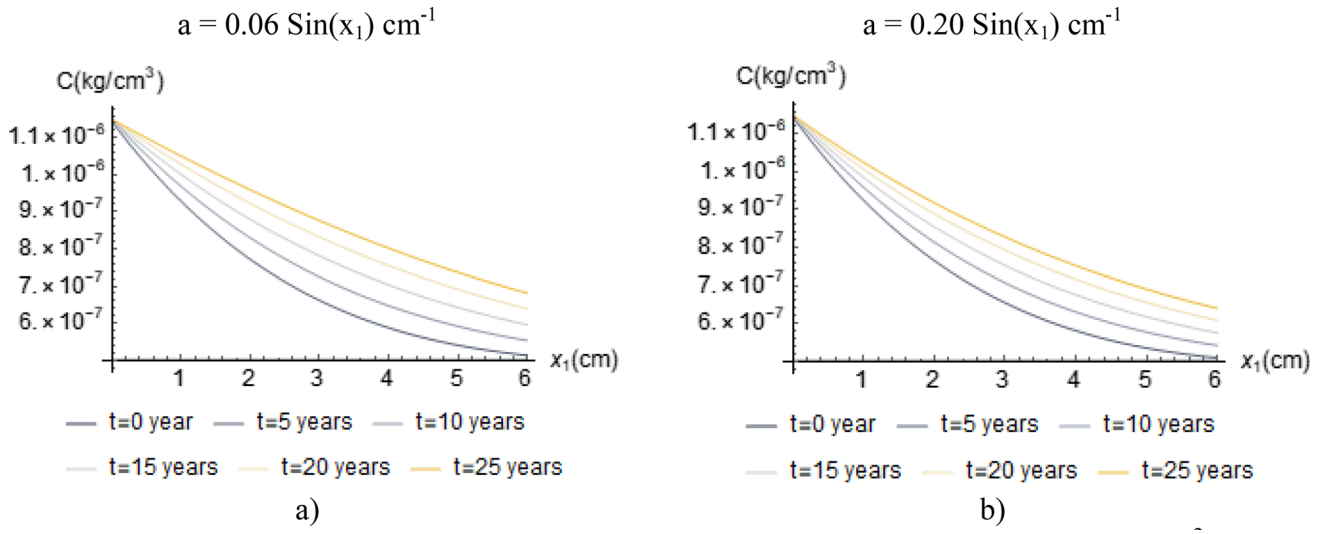

Fig. 8 1D electro-mechanical diffusion by using numerical solutions for $D_{cl} = 0.34$ cm^2/year, $a = 0.06\ \mathrm{Sin}(x_1)$ cm^{-1}, and $a = 0.20\ \mathrm{Sin}(x_1)$ cm.$^{-1}$

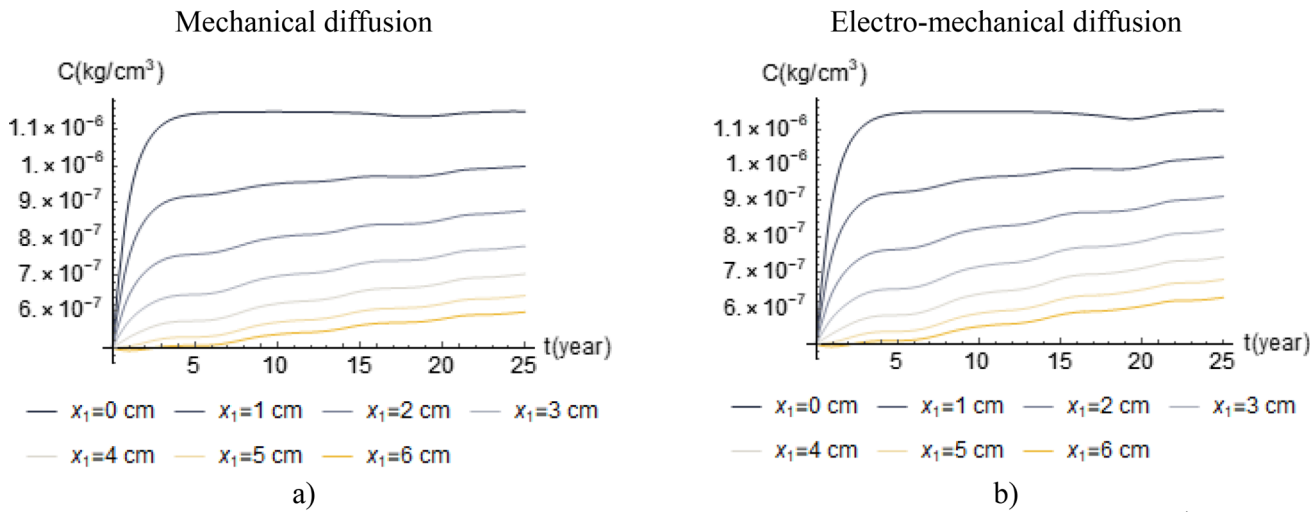

Fig. 9 1D diffusion using numerical solutions for D_{cl} Sin(t) for: **a** a = 0; **b** a = 0.13 cm.$^{-1}$

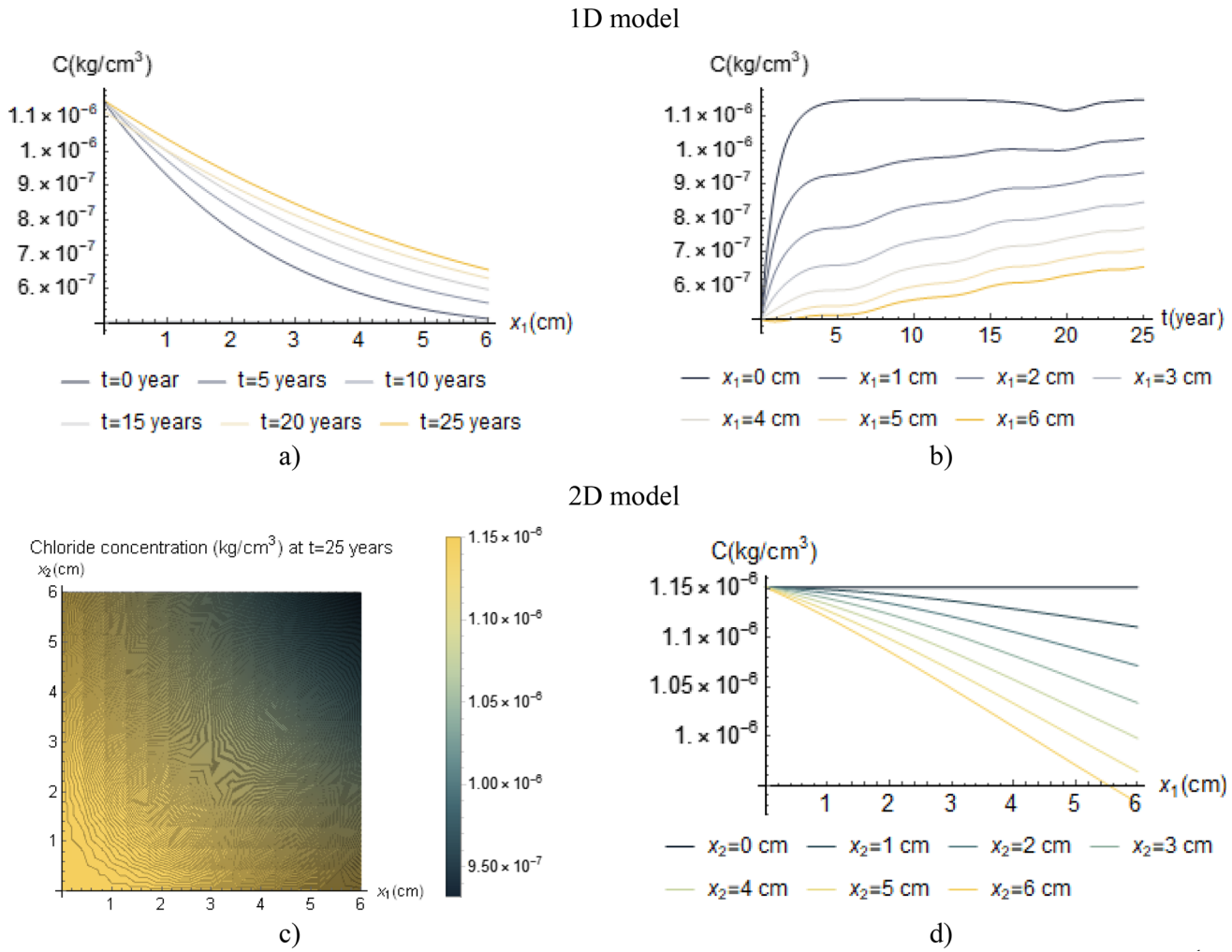

Fig. 10 1D/2D electro-mechanical diffusion by using numerical solutions for a = 0.13 cm^{-1} and D_{cl} = 0.34 cm^2/year

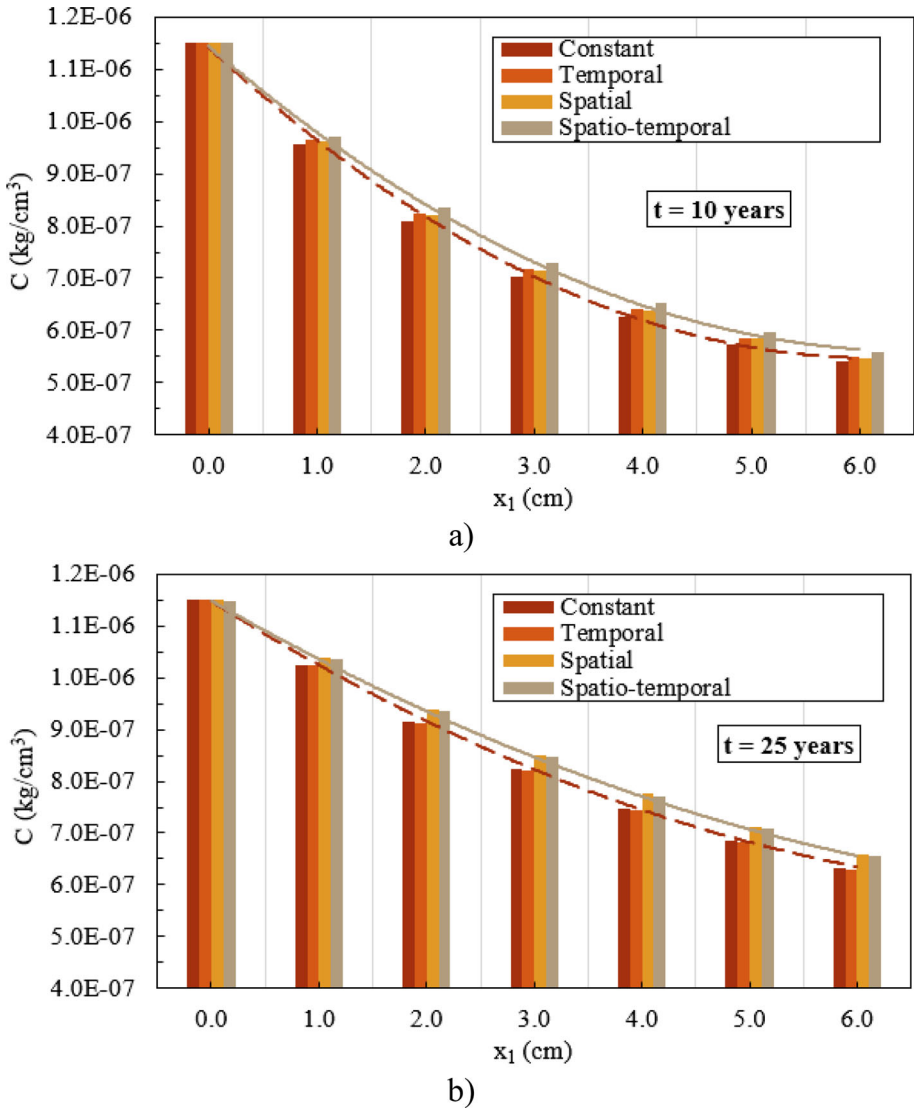

Fig. 11 Comparison between four models: **a** for t = 10.0 years and **b** for t = 25.0 years

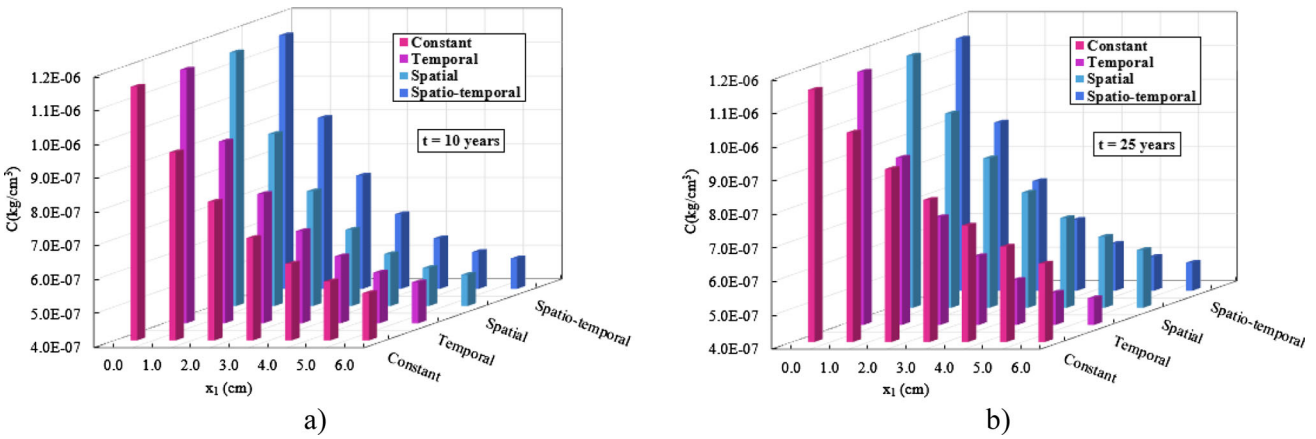

Fig. 12 Comparison between four models: **a** for t = 10.0 years and **b** for t = 25.0 years

Table 3 Comparison between some published studies and this analysis

Study	a-parameter (cm^{-1})	D_{cl} (cm^2/year) [a]	$\Gamma_{ratio} < 1.0$ [b]
[47]	23.77 *	2.64 *	0.36
[16]	15.85 *	6.16 *	0.71
[39]	13.86 *	0.33 *	0.24
[65]	23.77 *	2.71 *	0.41
This study	0.13 ± 0.07	0.34	0.85

* = Estimated value

[a] In the literature, the diffusivity is divided into intrinsic and apparent diffusivity, which are correlated by porosity and chloride binding [15, 49]. In this study, these aspects are covered in Eq. (9)

[b] Γ_{ratio} is calculated as the ratio between C values at $x_1 = 1.0$ cm and those at $x_1 = 0$ cm

and x_2. Figure 10 shows the electro-mechanical diffusion in the 1D/2D models.

Results in Fig. 10 show that the chloride concentration further increases by considering spatial and temporal variations. In the 2D model, the maximum values are higher than (~ 1.22) the values shown in Fig. 7c–d).

Figure 11 compares the results of chloride concentration C in x_1 of the four 1D models. It is possible to confirm that the chloride concentration with the constant parameters (dashed curve) is lower than that with spatial–temporal parameters (solid curve). This should indicate that the analytical solutions will not estimate the scenarios correctly.

Figure 12 compares the same four models as Fig. 11 but with some changes. The difference is that the sinusoidal functions shown in Fig. 3 have been translated downwards by 0.34. Thus, they have upper peaks coinciding with D_{cl}. This makes quantifying the fluctuation trends with positive and negative amplitudes possible. This could simulate, for instance, (i) internal convective flux of chloride ions with retrocession of the diffusion, (ii) possible interactions between different species (described in Sect. 4.1.2), and (iii) binding effects that decelerate the diffusion.

In this case, the chloride concentration with the constant parameters is higher than that with spatial–temporal parameters. In particular, for a lengthy period (e.g., $t = 25.0$ years), the chloride concentration for constant parameters (i.e., using analytical solutions) is somewhat overestimated. This indicates that analytical solutions should not be used to estimate relatively long-term scenarios.

5.2 Current/Diffusion/Deformation Correlations

Table 3 compares the results of this analysis with some studies published in the literature. The comparison focuses on the a-parameter, D_{cl}, and chloride concentrations (defined as a ratio between the concentration at $x_1 = 1.0$ cm and $x_1 = 0$ cm, i.e., $\Gamma_{ratio} < 1.0$). This ratio represents the available range to compare all studies since it could be difficult to standardize all results if a broad range is considered.

Although the results shown in Table 3 are provided by analyses that differ slightly from each other, it is still possible to discuss some aspects. This is because the key parameters of the electro-mechanical diffusion are E_k, thus a-parameter, and D_{cl}. Some results underestimate the chloride concentration (i.e., $\Gamma_{ratio} < 0.5$) concerning the analytical solutions that would provide, at $x_1 = 1.0$ cm, a value of $\Gamma_{ratio} \approx 0.80$. This is probably due to a poor calibration of the a-parameter in the published studies. For this, a stochastic approach proposed in this paper should provide better values for the a-parameter to reliably monitor chloride diffusion in RC structures.

Finally, in the literature [26, 45], there are some relations between ε_{kj} and the variation of I or resistance where a quasi-linear relation is shown. Similarly, some correlations between the a-parameter vs. f_5 and I vs. x_1 are estimated in Fig. 13.

The correlation in Fig. 13a) indicates a possible equilibrium between the concrete deformation ε_{kj}, the factor f_5, and the electric field quantified by the a-parameter. These curves could indicate how much it is necessary to vary ε_{kj} thus f_5 with respect to the a-parameter to individuate diffusivity D_{cl}, therefore a same chloride concentration C in concrete. Consequently, these bi-linear curves show a pair of values that rapidly estimate D_{cl} using Eq. (9) and concentration C using Eq. (12).

Figure 13b) shows a possible correlation between I and x_1. Under some conditions of the concrete these curves should indicate A_s and ρ (see Table 2) adopted in this paper, what is their current value at a certain depth x_1. The I values can be used to estimate the a-parameter (i.e., $I \rightarrow E_k \rightarrow a$). The upper curve is defined as $I + \sigma$ and the lower curve as $I-\sigma$, with a standard deviation $\sigma = 0.174$.

Figure 13 tries to correlate the current/diffusion/deformation, which is one goal of this paper. In this way, some values should be obtained to correlate electrical parameters (I and a) with mechanical/geometrical parameters (f_5 and x_1). In [16, 61], the conductivity, which is directly proportional to the electrical current I [24], increases as C increases. This could indicate that the conductivity and I increase as the electrical diffusivity increases.

6 Conclusions

The diffusion of electric-mechanical chloride ions in RC elements by non-constant multi-factorial diffusivity has been developed using advanced numerical solutions. The external ohmic and self-diffusion non-linear voltage distortion of multispecies have also been considered.

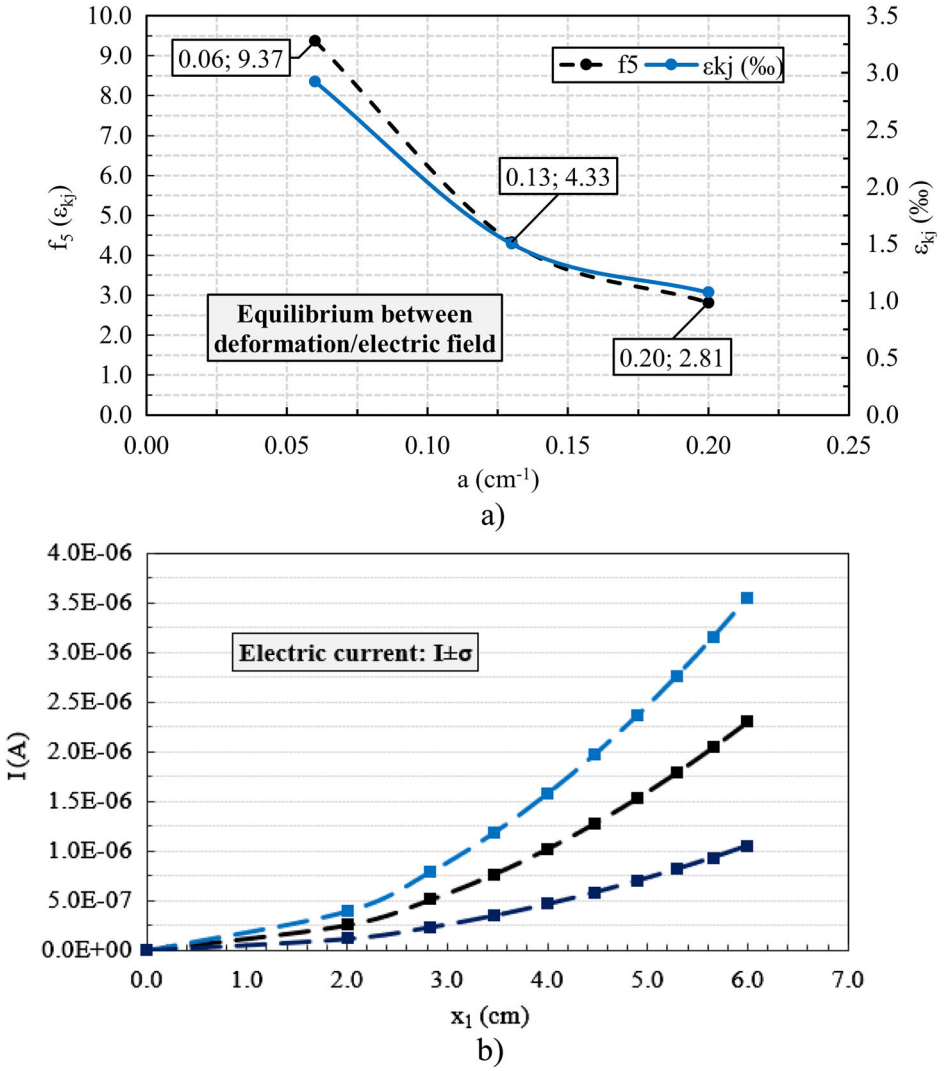

Fig. 13 Equilibrium between a) f_5 vs. a-parameter and b) I vs. x_1 (the upper curve is defined as I + σ and the lower curve as I-σ, with σ = 0.174 (Table 2))

The main conclusions are:

1. A multi-factorial diffusivity D_{cl} (Eq. (9)) has been defined to account for several factors that include the variable characteristics and external environmental context of the material (i.e., w/c ratio, binding chloride, temperature, concrete age, humidity, elastic deformation). Some of these factors are usually neglected when estimating the chloride concentration in RC elements; however, it is shown that they have an important role with a weight ranging from 3.0 to 99.0%. The elastic deformation factor, f_5, represents the "bridge" factor to justify the proposed current/diffusion/deformation model (Sect. 2.2).
2. The electrical field variation was estimated as the sum of the external ohmic and self-diffusion non-linear voltage distortion (Eq. (19)). The former corresponds to the external voltage applied to the concrete. In contrast, the latter is formed when the charged species start to move. The multispecies approach has thus been carried out under ~ 1100.0 simulations in an alternative probabilistic way. The a-parameter of the Nernst-Planck equation is estimated as 0.320 ± 0.174 V/m, which plays an important part in electrical–mechanical diffusion.
3. The analytical equation for electro-mechanical chloride ion diffusion (Eq. (12)) has been adapted to quantify the contribution of C_0 present in the concrete. Numerical solutions provided by HPs have been implemented to develop innovative results in 1D/2D directions. It has been shown that by considering a non-constant D_{cl} and a-parameter (i.e., spatial–temporal analysis), the chloride concentration in an RC element increases by up to 1.06 kg/m^3 (i.e., close to a moderate level of aggressiveness [54]). In general, it is difficult to predict the real contribution of the electro-mechanical mechanisms. Some correlations were also estimated, e.g., f_5 vs. a-parameter and I vs. x_1.

Acknowledgements The authors are grateful for support from the Project Mortar4Sewage (POCI-01-0247-FEDER-039829) funded by the Operational Program for Competitiveness and Internationalization (POCI) under Portugal 2020, with the support of the European Regional Development Fund (FEDER).

Funding Open access funding provided by FCT|FCCN (b-on).

Declarations

Conflict of interests None.

References

1. Lizarazo-Marriaga, J.; Higuera, C.; Guzmán, I.; Fonseca, L.: Probabilistic modelling to predict fly-ash concrete corrosion initiation. J Build Eng **30**, 1–8 (2020)
2. Nguyen, P.T.; Bastidas-Arteaga, E.; Amiri, O.; El Soueidy, C.P.: An efficient chloride ingress model for long-term lifetime assessment of reinforcement concrete structures under realistic climate and exposure conditions. Int J Concr Struct Mater **11**, 199–213 (2017)
3. Zhang, R.; Castel, A.; François, R.: Concrete cover cracking with reinforcement corrosion of RC beam during chloride-induced corrosion process. Cem. Concr. Res. **40**, 415–425 (2010)
4. Meira, G.R.; Andrade, M.C.; Padaratz, I.J.; Alonso, M.C.; Borba, J.C., Jr.: Measurements and modelling of marine salt transportation and deposition in a tropical region in Brazil. Atmos. Environ. **40**, 5596–5607 (2006)
5. Valdes, C., Castañeda, A., Corvo, F., Marrero, R., Montero, R.: Atmospheric corrosion study of carbon steel in Havana waterfront zone, In: Martirena-Hernandez J., Alujas-Díaz A., Amador-Hernandez M., Proceedings of the International Conference of Sustainable Production and Use of Cement and Concrete, RILEM Bookseries, 22, 1–10, Springer, Cham, 2020
6. Guerra, J.C.; Castañeda, A.; Corvo, F.; Howland, J.J.; Rodriguez, J.: Atmospheric corrosion of low carbon steel in a coastal zone of Ecuador: Anomalous behaviour of chloride deposition versus distance from the sea. Mater. Corros. **70**, 444–460 (2019)
7. Ou, Y.C.; Fan, H.D.; Nguyen, N.D.: Long-term seismic performance of reinforced concrete bridges under steel reinforcement corrosion due to chloride attack. Earthquake Eng. Struct. Dynam. **42**, 2113–2127 (2013)
8. Ye, H.; Fu, C.; Jin, N.; Jin, X.: Influence of flexural loading on chloride ingress in concrete subjected to cyclic drying-wetting condition. Comput. Concr. **15**, 183–199 (2015)
9. Farahani, A.; Taghaddos, H.; Shekarchi, M.: Prediction of long-term chloride diffusion in sílica fume concrete in a marine environment. Cement Concr. Compos. **59**, 10–17 (2015)
10. Zacchei, E.; Nogueira, C.G.: Chloride diffusion assessment in RC structures considering the stress-strain sate effects and crack width influences. Constr. Build. Mater. **201**, 100–109 (2019)
11. Fu, C.; Jin, X.; Ye, H.; Jin, N.: Theoretical and experimental investigation of loading effects on chloride diffusion in saturated concrete. J. Adv. Concr. Technol. **13**, 30–43 (2015)
12. Yari, A.; Mirnia, M.: Direct method for solution variational problems by using Hermite polynomials. Bol. Soc. Paran. Mat. **39**, 223–237 (2021)
13. Wang, Y., Wu, L., Wang, Y., Liu, C., Li, Q.: Effects of coarse aggregates on chloride diffusion coefficients of concrete and interfacial transition zone under experimental drying-wetting cycles, Construction and Building materials, pp. 230–245, 2018
14. Fu, C.; Ye, H.; Jin, X.; Jin, N.; Gong, L.: A reaction-diffusion modeling of carbonation process in self-compacting concrete. Comput. Concr. **15**, 847–864 (2015)
15. Carrara, P.; De Lorenzis, L.; Bentz, D.P.: Chloride diffusivity in hardened cement paste from microscale analyses and accounting for binding effects. Model. Simul. Mat. Sci. Eng. **24**, 1–44 (2016)
16. Claisse, P.A.; Elsayad, H.I.; Ganjian, E.: Modelling the rapid chloride permeability test. Cem. Concr. Res. **40**, 405–409 (2010)
17. Wang, X.H.; Bastidas-Arteaga, E.; Gao, Y.: Probabilistic analysis of chloride penetration in reinforced concrete subjected to pre-exposure static and fatigue loading and wetting-drying cycles. Eng. Fail. Anal. **84**, 205–219 (2018)
18. Truc, O.: Prediction of chloride penetration into saturated concrete-multi-species approach. Doktorsavhandlingar Vid Chalmers Tekniska Hogskola **1617**, 179 (2000)
19. ASTM International.: ASTM C1202–19, Standard test method for electrical indication of Concrete's ability to resist chloride ion penetration, 2019. West Conshohocken, PA
20. Marriaga, J.L.; Claisse, P.: Effect of the non-linear membrane potential on the migration of ionic species in concrete. Electrochim. Acta **54**(10), 2761–2769 (2009)
21. Das, S.; Saha, P.: A review of some advanced sensors used for health diagnosis of civil engineering structures. Measurement **129**, 68–90 (2018)
22. Cawley, P.: Structural health monitoring: Closing the gap between research and industrial deployment. Struct. Health Monit. **17**, 1225–1244 (2018)
23. Ferreira, A.D.B.L.; Nóvoa, P.R.O.; Marques, A.T.: Multifunctional material systems: a state-of-the-art review. Compos. Struct. **151**, 3–35 (2016)
24. D'Alessandro, A.; Meoni, A.; Ubertini, F.: Innovative composites with carbon nanofillers for self-sensing structural RC beams. Nano Hybrids Compos **19**, 12–22 (2018)
25. Ahmed, S.; Thostenson, E.T.; Schumacher, T.; Doshi, S.M.; McConnell, J.R.: Integration of carbon nanotube sensing skins and carbon fiber composites for monitoring and structural repair of fatigue cracked metal structures. Compos. Struct. **203**, 182–192 (2018)
26. Sanchez-Romate, X.F.; Artigas, J.; Jimenez-Suarez, A.; Sanchez, M.; Guemes, A.; Ureña, A.: Critical parameters of carbon nanotube reinforced composites for structural health monitoring applications: Empirical results versus theoretical predictions. Compos. Sci. Technol. **171**, 44–53 (2019)
27. Krishnaswamy, J.A.; Buroni, F.C.; Garcia-Sanchez, F.; Melnik, R.; Rodriguez-Tembleque, L.; Saez, A.: Lead-free piezocomposites with CNT-modified matrices: accounting for agglomerations and molecular defects. Compos. Struct. **224**, 1–15 (2019)
28. Zacchei, E.; Nogueira, C.G.: Calibration of boundary conditions correlated to the diffusivity of chloride ions: an accurate study for random diffusivity. Cement Concr. Compos. **1–14**, 2022 (2022)
29. Tadeu, A.; Simões, I.; Simões, N.; Prata, J.: Simulation of dynamic linear thermal bridges using a boundary element method model in the frequency domain. Energy Build. **43**, 3685–3695 (2011)

30. Cuenca, E.; D'Ambrosio, L.; Lizunov, D.; Tretjakov, A.; Volobujeva, O.; Ferrara, L.: Mechanical properties and self-healing capacity of ultra high performance fibre reinforced concrete with alumina nano-fibres: Tailoring ultra high durability concrete for aggressive exposure scenarios. Cement Concr. Compos. **118**, 1–17 (2021)
31. Liu, M.; Peng, L.; Huang, G.; Yang, Q.; Jiang, Y.: Simulation of stationary non-Gaussian multivariate wind pressures using moment-based piecewise Hermite polynomial model. J. Wind Eng. Ind. Aerodyn. **196**, 1–14 (2020)
32. Sun, Y.M.; Liang, M.T.; Chang, T.P.: Time/depth dependent diffusion and chemical reaction model of chloride transportation in concrete. App. Math. Mod. **36**, 1114–1122 (2012)
33. Zhang, S.F.; Lu, C.H.; Liu, R.G.: Experimental determination of chloride penetration in cracked concrete beams. Procedia Eng. **24**, 380–384 (2011)
34. Suo, Q.; Stewart, M.G.: Corrosion cracking prediction updating of deteriorating RC structures using inspection information. Reliab. Eng. Syst. Saf. **94**, 1340–1348 (2009)
35. Chen, W.; Zhang, J.; Zhang, J.: A variable-order time-fractional derivative model for chloride ions sub-diffusion in concrete structures. Fract. Calc. Appl. Anal. **16**, 76–92 (2013)
36. Kong, J.S.; Ababneh, A.N.; Frangopol, D.M.; Xi, Y.: Reliability analysis of chloride penetration in saturated concrete. Prob. Eng. Mech. **17**, 305–315 (2002)
37. Fan, W.J.; Wang, X.Y.: Prediction of chloride penetration into hardening concrete. Hind. Publis. Corp. **2015**, 1–8 (2015)
38. Fu C, Jin X, Jin N.: Modeling of chloride ions diffusion in cracked concrete. In: Earth and Space 2010: Engineering, Science, Construction, and Operations in Challenging Environments 3579–3589, 14–17 March, Honolulu, Hawaii, USA, 2010.
39. Tang, L., Nilsson, L.O.: Accelerated tests for chloride diffusivity and their application in prediction of chloride penetration, Materials Research Society Fall Meetings, Boston, Massachusetts, USA, 27/11–1/12, 1995.
40. Liu, J.; Ou, G.; Qiu, Q.; Chen, X.; Hong, J.; Xing, F.: Chloride transport and microstructure of concrete with/without fly ash under atmospheric chloride condition. Constr. Build. Mater. **146**, 493–501 (2017)
41. Bastidas-Arteaga, E.; Chateauneuf, A.; Sánchez-Silva, M.; Bressolette, P.; Schoefs, F.: A comprehensive probabilistic model of chloride ingress in unsaturated concrete. Eng. Struct. **33**, 720–730 (2011)
42. Zacchei, E.; Bastidas-Arteaga, E.: Multifactorial chloride ingress model for reinforced concrete structures subjected to unsaturated conditions. Buildings **12**, 1–22 (2022)
43. Liu, W.J.; Wang, Y.B.; Li, Q.B.; Gao, X.F.; Tan, Y.S.; Liu, C.F.; Hu, Y.; Niu, X.J.: Research on interlayer bonding quality control method of dam concrete based on equivalent age. Materials **14**, 1–14 (2021)
44. Gerard, B.; Pijaudier-Cabot, G.; Laborderie, C.: Coupled diffusion-damage modelling and the implications on failure due to strain localisation. Int. J. Solids Struct. **35**, 4107–4120 (1998)
45. Sanchez-Romate, X.F.; Garcia, C.; Rams, J.; Sanchez, M.; Ureña, A.: Structural health monitoring of a CFRP structural bonded repair by using a carbon nanotube modified adhesive film. Compos. Struct. **270**, 1–10 (2021)
46. Dinesh, A.; Sudharsan, S.T.; Haribala, S.: Self-sensing cement-based sensor with carbon nanotube: fabrication and properties–a review. Mater Today: Proc **46**, 5801–5807 (2021)
47. Lizarazo-Marriaga, J.; Claisse, P.: Modelling chloride penetration in concrete using electrical voltage and current approaches. Mater. Res. **14**, 31–38 (2011)
48. Zhang, Y.; Zhang, M.; Ye, G.: Influence of moisture condition on chloride diffusion in partially saturated ordinary Portland cement mortar. Mater. Struct. **51**, 1–18 (2018)
49. Da Costa, A.; Fenaux, M.; Fernández, J.; Sánchez, E.; Moragues, A.: Modelling of chloride penetration into non-saturated concrete: Case study application for real marine offshore structures. Constr. Build. Mater. **43**, 217–224 (2013)
50. Wu, L.; Wang, Y.; Wang, Y.; Ju, X.; Li, Q.: Modelling of two-dimensional chloride diffusion concentrations considering the heterogeneity of concrete materials. Constr. Build. Mater. **243**, 1–15 (2020)
51. Wolfram Mathematica 12, software version number 12.0, Wolfram Research, Inc., 2019.
52. Dattoli, G.: Generalized polynomials, operational identities and their applications. J. Comput. Appl. Math. **118**, 111–123 (2000)
53. Zacchei, E.; Nogueira, C.G.: 2D/3D numerical analyses of corrosion initiation in RC structures accounting fluctuations of chloride ions by external actions. KSCE J. Civ. Eng. **1–16**, 2021 (2021)
54. El Hassan, J.; Bressolette, P.; Chateauneuf, A.; El Tawil, K.: Reliability-based assessment of the effect of climatic conditions on the corrosion of RC structures subject to chloride ingress. Eng. Struct. **32**, 3279–3287 (2010)
55. Rodriguez, R.G.; Aperador, W.; Delgado, A.: Calculation of chloride penetration profile in concrete structures. Int. J. Electrochem. Sci. **8**, 5022–5035 (2013)
56. Imounga, H.M.; Bastidas-Arteaga, E.; Pitti, R.M.; Ango, S.E.; Wang, X.H.: Bayesian assessment of the effects of cyclic loads on the chloride ingress process into reinforced concrete. Appl. Sci. **10**, 1–19 (2020)
57. N.T. Nordtest.: BUILD 492, Concrete, mortar and cement-based repair materials: chloride migration coefficient from non-steady-state migration experiments, 1999
58. Lizarazo-Marriaga, J.; Claisse, P.: Determination of the concrete chloride diffusion coefficient based on an electrochemical test and an optimization model. Mater. Chem. Phys. **117**, 536–543 (2009)
59. Vanýsek, P.: Ionic conductivity and diffusion at infinite dilution, Handbook of Chemistry and Physics, 1992/93 edition, p. 77–79. CRC Press, Boca Raton (1992)
60. Dalziel, C.F.; Lee, W.R.: Reevaluation of lethal electric currents. IEEE Trans. Ind. Gener. Appl. **5**, 467–476 (1968)
61. Kim, H.K.: Chloride penetration monitoring in reinforced concrete structure using carbon nanotube/cement composite. Constr. Build. Mater. **96**, 29–36 (2015)
62. Rodríguez-Tembleque, L.; García-Sánchez, F.; Sáez, A.: Crack-face frictional contact modelling in cracked piezoelectric materials. Comput. Mech. **64**, 1655–1667 (2019)
63. W.J. Fan, X.Y. Wang, Prediction of Chloride Penetration into Hardening Concrete, Hind. Publis. Corp., pp. 1–8, 2015
64. Kim, Y.Y., Lee, B.J., Kwon, S.J.: Evaluation technique of chloride penetration using apparent diffusion coefficient and neural network algorithm, Advances in Materials Science and Engineering, pp. 1–13, 2014
65. Marriaga, J.L.; Claisse, P.: The influence of the blast furnace slag replacement on chloride penetration in concrete. Ingeniería e Investigación **31**, 38–47 (2011)